AMERICAN ACADEMY OF OPHTHALMOLOGY®

Measuring Glaucomatous Focal Perfusion Loss in the Peripapillary Retina Using OCT Angiography

Aiyin Chen, MD, Liang Liu, MD,* Jie Wang, MS, Pengxiao Zang, MS, Beth Edmunds, MD, PhD, Lorinna Lombardi, MD, Ellen Davis, MD, John C. Morrison, MD, Yali Jia, PhD, David Huang, MD, PhD*

Purpose: To measure low perfusion areas (LPAs) and focal perfusion loss (FPL) in the peripapillary retina using OCT angiography (OCTA) in glaucoma.

Design: Prospective, observational study.

Participants: A total of 47 patients with primary open-angle glaucoma (POAG) and 36 normal participants were analyzed.

Methods: One eye of each subject was scanned using an AngioVue (Optovue, Fremont, CA) 4.5-mm OCTA scan centered on the disc. En face nerve fiber layer (NFL) plexus angiogram was generated. With the use of custom software, a capillary density map was obtained by computing the fraction of area occupied by flow pixels after low-pass filtering by local averaging 21×21 pixels. The low-perfusion map is defined by local capillary density below 0.5 percentile over a contiguous area above 98.5 percentile of the normal reference population. The LPA parameter is the cumulative area, and the FPL is the percent capillary density loss (relative to normal mean) integrated over the LPA.

Main Outcome Measures: Peripapillary retinal LPA and FPL.

Results: Among patients with POAG, 3 had preperimetric glaucoma and 44 had perimetric glaucoma, with visual field (VF) mean deviation (MD) of −5.14±4.25 decibels (dB). The LPA was 3.40±2.29 mm^2 in those with POAG and 0.11±0.18 mm^2 in normal subjects ($P < 0.001$). The FPL was 21.8%±17.0% in those with POAG and 0.3%±0.7% in normal subjects ($P < 0.001$). The diagnostic accuracy as measured by the area under the receiver operating curve was 0.965 for both LPA and FPL, with a sensitivity of 93.7% at 95% specificity. The repeatability as measured by intraclass correlation coefficient was 0.977 for LPA and 0.958 for FPL. The FPL had excellent correlation with VF MD (Spearman's rho = −0.843), which was significantly ($P = 0.008$) better than the correlation between NFL thickness and VF MD (rho = 0.760). The hemispheric difference correlation between FPL and VF (Spearman's rho = 0.770) was significantly ($P < 0.001$) higher than the hemispheric difference correlation between LPA and VF (rho = 0.595).

Conclusions: The low-perfusion map and LPA and FPL parameters are able to assess the location and severity of focal glaucoma damage with good agreement with VF. *Ophthalmology 2020;127:484-491 © 2019 by the American Academy of Ophthalmology*

Glaucoma is the leading cause of irreversible blindness worldwide and is projected to affect 111.8 million people by 2040.[1] Because of its irreversible nature, early diagnosis, prompt treatment, and careful monitor for changes are keys to prevent progression and blindness. Visual field (VF) and OCT are 2 essential modalities for glaucoma assessment, but each has its limitations. Visual field directly assesses function, but the testing is subjective, time-consuming, and poorly reproducible.[2,3] OCT measures the nerve fiber layer (NFL) in the peripapillary retina and the ganglion cell complex in the macula. It provides a more objective assessment of structural abnormalities in glaucoma.[4] Structural OCT has been shown to detect perimetric glaucoma well[5-8] and is more sensitive than VF for detecting progression trend in the early stages of glaucoma.[9] However, structural OCT parameters have important limitations. They have only moderate sensitivity in detecting glaucoma in its early stage.[10,11] They do not correlate well with VF parameters.[12] In the later stages of glaucoma, structural measures approach floor values and cease to be reliable measures of glaucoma progression.[13-15] Therefore, a novel diagnostic technology that overcomes some of the limitations of VF and structural OCT could potentially improve clinical glaucoma evaluation.

OCT angiography (OCTA) is a noninvasive imaging modality that uses intrinsic motion contrast to detect blood flow down to the capillary level. OCTA has been used to detect perfusion loss in the optic disc,[16,17] peripapillary retina,[18-21] and macula.[20,22,23] OCTA parameters such as vessel density, capillary density, and flow index have been found to have good diagnostic accuracy for glaucoma[18,24,25] and correlate

© 2019 by the American Academy of Ophthalmology
Published by Elsevier Inc.
https://doi.org/10.1016/j.ophtha.2019.10.041
ISSN 0161-6420/19

well with VF parameter.[21,23,26] These previously described OCTA parameters are sensitive to global and regional diffuse loss but not particularly suited to detecting focal loss. Previous experience in VF and structural OCT analysis has taught us that focal loss analysis could provide valuable complementary information for glaucoma evaluation. Early glaucoma damage is often concentrated in a small area in a characteristic pattern; thus, a map of focal damage could provide earlier detection and differentiation from other conditions (i.e., cataract, myopia, retinal diseases).[27-29] Focal loss analysis in OCT was found to be particularly powerful in predicting future glaucoma progression.[30,31] Thus, it is desirable to also develop methods for focal perfusion analysis using OCTA. In this study, we developed a novel OCTA image processing algorithm to map and quantify focal perfusion defects associated with glaucoma. The resulting focal perfusion parameters were evaluated in a small cross-sectional study of patients with glaucoma and normal subjects.

Methods

Study Population

This prospective observation study was performed from March 6, 2015, to June 21, 2017, at the Casey Eye Institute, Oregon Health & Science University. The research protocols were approved by the Institutional Review Board at Oregon Health & Science University and carried out in accordance with the tenets of the Declaration of Helsinki. Written informed consent was obtained from each participant.

All participants were part of the "Functional and Structural Optical Coherence Tomography for Glaucoma" study (R01 EY023285). The inclusion criteria for the perimetric glaucoma group were (1) an optic disc rim defect (thinning or notching) or retinal NFL defect visible on slit-lamp biomicroscopy and (2) a consistent glaucomatous pattern, on both qualifying Humphrey Swedish Interactive Thresholding Algorithm 24-2 VFs, meeting at least 1 of the following criteria: pattern standard deviation outside normal limits ($P < 0.05$) or glaucoma hemifield test outside normal limits. Eyes in the preperimetric glaucoma group must meet both of the following criteria: (1) an optic nerve with glaucomatous defect or retinal NFL bundle defect based on slit-lamp examination and (2) no evidence of VF loss consistent with glaucoma.

For the normal group, the inclusion criteria were (1) no evidence of retinal pathology or glaucoma; (2) a normal Humphrey 24-2 VF; (3) intraocular pressure <21 mmHg; (4) central corneal pachymetry >500 μm; (5) no chronic ocular or systemic corticosteroid use; (6) an open angle on gonioscopy; (7) a normal appearing optic nerve head (ONH) and NFL; and (8) symmetric ONH between left and right eyes.

The exclusion criteria for both groups were (1) best-corrected visual acuity less than 20/40; (2) age <40 or >80 years; (3) spherical equivalent refractive error of >+3.00 diopters (D) or <−7.00 D; (4) previous intraocular surgery except for an uncomplicated cataract extraction with posterior chamber intraocular lens implantation; (5) any diseases that may cause VF loss or optic disc abnormalities; or (6) inability to perform reliably on automated VF testing. One eye from each participant was scanned and analyzed. For normal eyes, the eye was randomly selected. For the preperimetric glaucoma and perimetric glaucoma group, the eye with the worse VF was selected.

Visual Field Testing

Visual field tests were performed with the Humphrey Field Analyzer II (Carl Zeiss, Inc, Oberkochen, Germany) set for the 24-2 threshold test, size III white stimulus, using the Swedish Interactive Thresholding Algorithm. The VF mean deviation (MD), VF pattern standard deviation, and VF index were used to calculate the correlations with OCTA parameters.

OCT

A 70-kHz, 840-nm wavelength spectral-domain OCT system (Avanti RTVue-XR, Optovue Inc, Fremont, CA) was used.

Image Acquisition and Processing

The peripapillary retinal region was scanned using a 4.5×4.5-mm volumetric angiography scan centered on fixation. Each volume was composed of 304 line-scan locations at which 2 consecutive B-scans were obtained. Each B-scan contained 304 A-scans. The AngioVue software used the split-spectrum amplitude-decorrelation angiography algorithm,[32] which compared the consecutive B-scans at the same location to detect flow using motion contrast.[32] Each scan set was composed of 2 volumetric scans: 1 vertical-priority raster and 1 horizontal-priority raster. The AngioVue software used an orthogonal registration algorithm to register the 2 raster volumes to produce a merged 3-dimensional OCT angiogram.[33] This reduces motion artifacts and improves image quality.[34] Two sets of scans were performed within 1 visit.

The merged volumetric angiograms were then exported for custom processing using the Center for Ophthalmic Optics & Lasers-Angiography Reading Toolkit software.[35] The OCTA scans contained both volumetric flow (decorrelation) data and structural (reflectance) data. Segmentation of the retinal layers was performed by automated MATLAB programs (MathWorks, Natick, MA) that operate on the structural OCT data. Further manual correction of the segmentation was conducted if required. An en face angiogram of retinal nerve fiber layer plexus (NFLP) was obtained by maximum flow (decorrelation value) projection. The Center for Ophthalmic Optics & Lasers-Angiography Reading Toolkit removed flow projection artifacts and calculated reflectance-compensated capillary density (CD). The vessel density, defined as the percentage area occupied by the large vessels and microvasculature, was evaluated in the 4×4-mm scan area excluding the central 2-mm diameter circle, which was manually centered on the optic disc based on the en face reflectance image. Arterioles and venules (larger vessels) were automatically identified by thresholding the en face mean projection of OCT reflectance within the all-plexus slab. After these larger vessels were excluded, the remaining angiogram was used to compute CD. With the use of custom software, a CD map was obtained by computing the fraction of area occupied by flow pixels after low-pass filtering 21×21-pixel elements. Low perfusion was first defined by CD below the 0.5 percentile threshold in the normal reference eyes. Contiguous pixels with low perfusion were grouped to measure the contiguous low perfusion areas. The distribution of contiguous low perfusion areas in normal eyes were examined, and its 98.5 percentile cutoff point was 0.053 mm^2. The binary low-perfusion map highlighted areas of normal perfusion in green and abnormally low perfusion area in red. The low perfusion area (LPA) in each eye was defined by the cumulative area of pixels that met both low perfusion and contiguity requirements. The focal perfusion loss (FPL) is the capillary density loss (relative to the reference map from a normal population) integrated over the LPA then expressed as a percentage of the capillary density integral of the normal reference map. The LPA and FPL were measured from the

4×4-mm low-perfusion map, which were global OCTA parameters. To facilitate FPL and VF loss correspondence, LPA and FPL were divided into superior and inferior hemispheric values by a horizontal line crossing the center of the optic disc.

Because we found OCTA measurements to be strongly correlated with signal strength index in previous studies, we developed a reflectance-adjustment method that corrected the artifactually lower flow signal in regions of reduced reflectance (e.g., due to media opacity or pupil vignetting).[36] Clinical validation showed that this algorithm was able to remove the dependence of retinal OCTA measurements on the signal strength index and reduce population variation.[23,36]

Image quality was assessed for all OCTA scans. Poor-quality scans with signal strength index below 50 and registered image sets with residual motion artifacts (discontinuous vessel pattern) were excluded from analysis. Two image sets, each meeting the quality criteria, were required to provide data for an assessment of within-visit repeatability. These were then averaged for further analysis. Within-visit repeatability was assessed by the pooled standard deviation and the intraclass correlation coefficient.

Structural OCT Analysis

Peripapillary NFL thickness was measured from the ONH scan. The ONH concentric (1.3−4.9 mm diameter) scans were centered on the optic disc. In postprocessing, the ONH scan was automatically registered with a baseline 3-dimensional disc scan to provide the disc margin information. The NFL thickness profile at a diameter of 3.4 mm was resampled on the NFL thickness map recentered according to the detected optic disc center. The result for each participant was the average value of 2 sets of images obtained at 1 visit.

Statistical Analysis

The Student *t* test was used to compare normal and glaucoma groups. Mean ocular perfusion pressure = 2/3*mean arterial pressure − intraocular pressure, where mean arterial pressure = 2/3*diastolic blood pressure + 1/3*systolic blood pressure. Pearson correlation was used to determine the relationships between LPA and FPL with the traditional glaucoma measurements of function and structure, such as the VF MD and circumpapillary retinal NFL thickness. All statistical analyses were performed with SPSS 20.0 (SPSS Inc, Chicago, IL) and MedCalc 10.1.3.0 (MedCalc Software, Ostend, Belgium, www.medcalc.be). The Cohen's kappa coefficient is used to measure the localization correspondence between FPL and VF. The area under the receiver operating characteristic curve, sensitivity, and specificity were used to evaluate diagnostic accuracy. The estimated sensitivities for fixed specificities were calculated by MedCalc software using the method of Zhou et al.[37] The McNemar test was used to compare sensitivities of parameters. The statistical significance was assumed at $P < 0.05$.

Results

Study Population

Peripapillary retinal perfusion was studied in 39 normal and 50 glaucoma participants. Three normal and 3 glaucoma participants were not analyzed because of poor OCTA scan quality, leaving 36 normal and 47 glaucoma participants for statistical analysis (Table 1). In the glaucoma group, 3 participants had preperimetric glaucoma, 27 participants had early glaucoma, 14 participants had moderate glaucoma, and 3 participants had severe glaucoma, according to the modified classification system by Hodapp et al.[38] A total of 45 patients with glaucoma were using at least 1 glaucoma drop. There was no statistically significant difference between the normal and glaucoma groups for age, intraocular pressure, mean ocular perfusion pressure, and systolic/diastolic blood pressures (Table 1). As expected, glaucoma participants had significantly worse VF and structural OCT parameters. The LPA and FPL were not correlated with age or signal strength index in the normal group ($P > 0.23$).

Qualitative Assessment of Focal Capillary Dropout

In the normal eye (Fig 1), the NFLP angiogram showed that the capillary density was greater along the superotemporal and inferotemporal arcuate nerve fiber bundles. There was no LPA or VF defect. A perimetric glaucoma eye was chosen to demonstrate the loss of retinal capillaries in both the superior and inferior hemispheres in comparison with the normal eye (Fig 1). In the glaucomatous eye, severe capillary dropout with a wedge pattern in the superior hemisphere could be clearly visualized in both the NFLP angiogram and low-perfusion map. However, in the inferior hemisphere, the low-perfusion map showed another wedge-shaped region of capillary dropout that was only partially visible in the NFLP angiogram and density map. In the nasal region of this glaucomatous eye, both the NFLP angiogram and capillary density map showed an area of low capillary density. The low-perfusion map showed that the low capillary density was within normal, because the nasal sector normally has lower capillary density. The LPA in the superior and inferior arcuate regions matched well with the VF defects in this glaucomatous eye. Overall, the low-perfusion map provided more clear and reliable visualization of focal glaucomatous defect. We analyzed the low-perfusion map in each eye and found that among the 47 glaucomatous eyes, 32 eyes have wedge-shaped low perfusion areas extending to the disc similar to the example in Figure 1, 4 eyes have wedge patterns plus scattered low perfusion areas not associated with the wedge patterns, 8 eyes have diffuse capillary dropout, and only 1 eye has peripheral low perfusion areas without extending to the disc. This case (preperimetric glaucoma) was associated with a normal VF. Thus, a majority of the low perfusion areas have patterns consistent with glaucoma damage. A total of 39 of the 47 glaucomatous eyes and all 36 of the normal eyes have areas of suspicious capillary dropout in the NFLP angiogram, which were found to be normal on the LPA map. Most of these areas were located at the nasal quadrant similar to what is demonstrated in Figure 1. Therefore, the low-perfusion map was more reliable than inspection of the raw angiogram in distinguishing glaucomatous changes in capillary density from normal variations.

Localization of Focal Perfusion Loss with Visual Field Loss

In glaucomatous eyes, we expected those with worse perfusion in the superior hemisphere to have worse inferior VF loss and those with worse perfusion in the inferior hemisphere to have worse superior VF loss. We tested this hypothesis in the 38 perimetric glaucomatous eyes that had a significant superior-inferior hemispheric difference in VF deviation, defined as hemispheric differences outside of the 95% confidence interval found in the normal group, which was +1.44 decibels (dB) to −1.07 dB. In 36 eyes, the worse hemisphere matched for VF and OCTA FPL. There was mismatch in 2 eyes. Thus, there was good agreement between VF and FPL (Cohen's kappa 0.88; 95% confidence interval, 0.71−1) in the hemispheric location of worse damage. The agreement was only moderate

Table 1. Participants' Characteristics

Parameter	Normal	Glaucoma	Difference (*P* Value)
Participants, n	36	47	
Eyes, n	36	47	
Age (yrs)	65±8	66±9	1 (0.530)
Glaucoma medications	0	2±1	
Intraocular pressure (mmHg)	15.4±2.7	14.9±3.1	−0.5 (0.375)
Diastolic blood pressure (mmHg)	78.6±10.8	77.8±10.8	−0.8 (0.959)
Systolic blood pressure (mmHg)	126.4±16.2	125.2±15.6	−1.2 (0.804)
Mean ocular perfusion pressure (mmHg)	47.7±7.3	47.5±6.9	−0.2 (0.707)
BCVA (logMAR)	0.00±0.10	0.03±0.11	0.03 (0.271)
Cataract (0–4)	0.8±0.9	1.5±0.8	0.7 (0.03)
VF			
MD (dB)	0.09±1.14 (−3.22–1.87)	−5.14±4.25 (−17.6–0.53)	−5.23 (<0.001)
PSD (dB)	1.42±0.25 (1.02–2.17)	6.54±4.02 (1.51–14.46)	5.12 (<0.001)
Structural OCT thickness measurement			
NFL (μm)	98.2±7.0 (85∼111)	75.3±12.6 (54∼106)	−22.8 (<0.001)
OCTA Measurements			
Low perfusion area (mm^2)	0.11±0.18 (0–0.61)	3.40±2.29 (0–9.89)	3.29 (<0.001)
FPL (%)	0.3±0.7 (0–3.0)	21.8±17.0 (0–82.8)	21.5 (<0.001)

BCVA = best-corrected visual acuity; dB = decibels; FPL = focal perfusion loss; logMAR = logarithm of the minimum angle of resolution; MD = mean deviation; NFL = nerve fiber layer; OCTA = OCT angiography; PSD = pattern standard deviation; VF = visual field.
Statistical significance tested by 2-tailed *t* test. The combination agents were counted as 2 medications.
Numbers displayed are mean ± standard deviation (range).

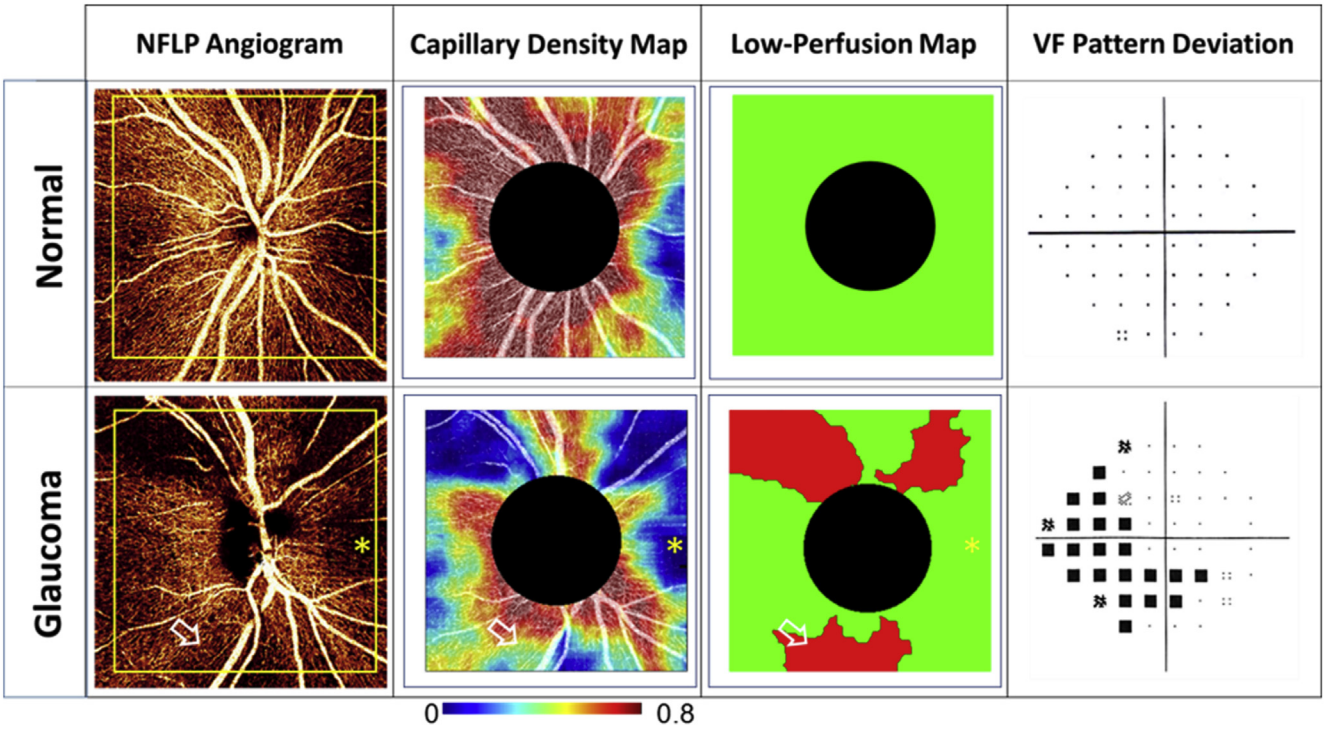

Figure 1. Mapping of capillary density in the nerve fiber layer plexus (NFLP) was demonstrated on 4.5-mm OCT angiography (OCTA) scans of a normal eye and glaucomatous eye. The glaucomatous eye had lower capillary density in general on capillary density map and showed the arcuate patterns of focal loss on the low perfusion area (LPA). The low-perfusion map provided more accurate identification of the locations of focal loss than the angiogram or capillary density map. An area of low capillary density (*) was found to be normal for the nasal region on LPA analysis. However, although capillaries are clearly visible in the inferior arcuate area (**arrow outline**), the density was found to be abnormally low in LPA analysis. In this moderate glaucomatous eye with visual field (VF) mean deviation (MD) of −11.4 decibels (dB), the low perfusion area was 4.6 mm^2 and the focal perfusion loss (FPL) was 29%.

Table 2. Diagnostic Accuracy of Nerve Fiber Layer Plexus Capillary Density, Low Perfusion Area, and Focal Perfusion Loss

Global Parameters	AROC	Sensitivity* (95% CI)
LPA	0.965	93.7% (82.5%–98.7%)
FPL	0.965	93.7% (82.5%–98.7%)
NFLP CD	0.947	80.9% (66.7%–90.9%)

AROC = area under the receiver operating characteristic curve; CI = confidence interval; FPL = focal perfusion loss; LPA = low perfusion area.
*Sensitivities were evaluated at the 95% specificity cutoff.

between VF and LPA (Cohen's kappa 0.62; 95% confidence interval, 0.37–0.86).

The superior-inferior hemispheric differences for FPL were strongly correlated with the superior-inferior hemifield differences in VF deviation (Spearman's rho = 0.770, $P < 0.001$). The hemispheric difference correlation between LPA and VF was significantly ($P < 0.001$) lower (Spearman's rho = 0.595, $P < 0.001$).

Overall, the hemispheric asymmetry analyses showed that FPL may be a better indicator of the severity of regional glaucoma damage than LPA in terms of correspondence with VF.

Glaucoma Diagnostic Accuracy and Correlation with Traditional Glaucoma Diagnostic Measurements

Both LPA and FPL (global values) were significantly lower in the glaucoma group, compared with the normal group (Table 1). The LPA and FPL had the same glaucoma diagnostic accuracies as judged by the sensitivity at 95% specificity and area under the receiver operating characteristic curve for differentiating 36 normal and 47 glaucoma participants (Table 2). The FPL and LPA have higher diagnostic accuracy (area under the receiver operating characteristic curve) and sensitivity compared with global NFLP CD (Table 2), but the advantage was only statistically significant ($P = 0.016$) for the sensitivity.

The FPL and LPA had good correlations with VF parameters (MD, pattern standard deviation, and VF index) and structural OCT overall NFL thickness (Table 3). These correlations were all highly significant. The FPL had excellent correlation with VF MD (Spearman's rho = −0.843), which was significantly ($P = 0.008$) better than the correlation between NFL thickness and MD (rho = 0.760). This showed that OCTA parameters may be better indicators of glaucoma severity than structural OCT parameters, in terms of correlation with VF.

Because FPL takes into account the depth of capillary loss and its area, it may be a more complete measure of glaucoma damage than LPA. We found that FPL was better than LPA in terms of correlation with VF parameters (Table 3), but the advantage was not statistically significant. On individual examples, we see that although the low-perfusion map locates focal capillary dropout, the FPL parameter better quantifies the severity of focal damage (Fig 2).

Repeatability in Glaucoma Group

In 47 glaucoma participants, the FPL and LPA had excellent within-visit repeatability. The intraclass correlation coefficients of FPL and LPA were 0.958 and 0.977, respectively. The pooled standard deviation of FPL and LPA were 3% and 0.3 mm^2, respectively.

Table 3. Spearman Correlation Matrix of Low Perfusion Area, Focal Perfusion Loss, Visual Field Parameters, and Structural Variables

Parameters	FPL	LPA	VF MD	VF PSD	VFI
LPA	0.989				
VF MD	−0.843	−0.825			
VF PSD	0.818	0.797	−0.878		
VFI	−0.884	−0.861	0.876	−0.930	
NFL thickness	−0.841	-0.851	0.760	−0.716	0.753

FPL = focal perfusion loss; LPA = low perfusion area; NFL = nerve fiber layer; VFI = visual field index; VF MD = visual field mean deviation; VF PSD = visual field pattern standard deviation.
Glaucoma and normal groups were both included in this analysis. Spearman's rho are shown. All P values < 0.001.

Discussion

In this study, we describe a novel OCTA analysis that maps areas of significant perfusion loss (the low-perfusion map) and 2 novel OCTA parameters that quantify cumulative area of reduced perfusion as LPA and severity of the perfusion loss as FPL. Both LPA and FPL are significantly higher in primary open-angle glaucoma (POAG) compared with normal eyes, with good repeatability and high sensitivity and specificity. Although LPA shows the size of the area with abnormally low perfusion, FPL denotes the severity of the loss in vessel density. Our study agrees with others that OCTA shows reduced microvasculature in peripapillary retina in glaucomatous eyes.[18,25,39]

One challenge of OCTA is that certain areas may normally have higher vessel density and other areas may have less.[40] Therefore, it is necessary to develop an algorithm to compare an area of question with a normative database to distinguish areas with statistically significant loss of perfusion (abnormally low perfusion) from areas where the perfusion is normally lower than other areas (e.g., nasal region). The low-perfusion map is a binary map highlighting areas of normal perfusion in green and abnormally low perfusion area in red. This allows the clinician to easily correlate areas of significant perfusion loss with area of significant NFL thinning, which are conveniently marked in red in most commercial software. Correlation with areas of significant VF loss is also possible using the known sector correspondence between VF area and NFL profile.[41,42]

Regarding structural correlation, both LPA and FPL correlate well with OCT overall NFL thickness. The association between peripapillary OCTA vessel density with NFL thickness has been well documented in other studies,[18,25,43] and our findings came as no surprise. Perfusion loss and NFL thinning are both associated with POAG.

In terms of functional correlation, LPA and FPL both correlated well with VF defects in global and hemispheric analyses. Our finding agrees with several studies that have demonstrated the association between vessel density and VF global and hemispheric abnormalities.[17,18,26,44] For example, Yarmohammadi et al[45] studied subjects who have VF defects confined to 1 hemisphere and found the mean peripapillary vessel density to be lowest in the affected hemi-

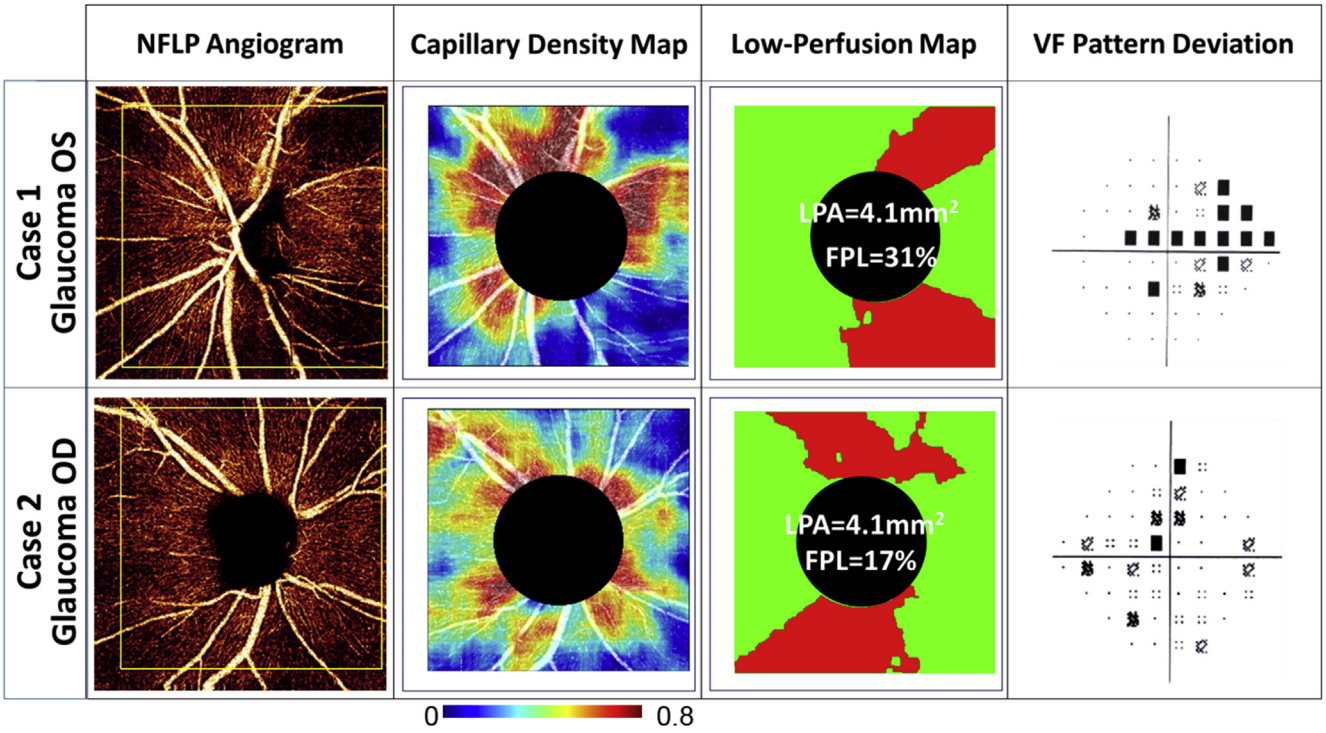

Figure 2. Two glaucomatous eyes from different patients are shown as examples of quantitative FPL analysis. The 2 eyes had the same overall LPA −4.1 mm^2. Case 1 had more FPL (31%) than case 2 (FPL 17%), which matched with its larger VF defects. The inferior hemispheres have worse FPL in both cases, which matched with the superior locations of worse hemifields. FPL = focal perfusion loss; LPA = low perfusion area; NFLP = nerve fiber layer plexus; VF = visual field.

retina. Richter et al[44] similarly found superior and inferior VF MD associated with corresponding OCTA parameters. In POAG eyes with hemispheric VF defect, Chen et al[19] found reduced NFL microcirculation even in the hemisphere without the field defect compared with eyes without glaucoma. In our study, FPL correlates better with VF loss than LPA, which is expected because LPA only measures the area of perfusion loss, whereas FPL also accounts for the depth of perfusion loss and is a more complete measure of the severity of glaucoma damage. In our study, the correlation between FPL and VF MD was significantly higher than the correlation between NFL thickness and VF MD. This agrees with previous studies that generally found OCTA vessel density to be better than NFL thickness in terms of correlation with VF parameters.[21,26] Results from this study and the literature both support that perfusion-function correlation is higher than structure-function correlation. One possible interpretation of this finding is that structure only measures the loss of retinal ganglion cell, whereas both function and perfusion also assess the presence of dysfunctional ganglion cells. Low perfusion could be a cause or sequelae of ganglion cell dysfunction, which could only be resolved with interventional studies.

Study Limitations

There are several limitations of the study. This is a cross-sectional study; therefore, the use of LPA and FPL in the prediction and monitoring for glaucoma progression cannot be assessed. Previous OCT studies have found that focal ganglion cell complex and NFL thinning are the best structural predictors of future glaucoma damage.[30,31,46] Therefore, our novel FPL parameters are promising candidates for a longitudinal study on predicting which patients are likely to experience rapid glaucoma progression. Another limitation of our study is the small number of patients with preperimetric glaucoma. Therefore, despite the excellent diagnostic accuracy shown, we cannot make a conclusion regarding the potential efficacy of LPA and FPL in improving the early diagnosis of glaucoma. Our preperimetric glaucoma group was defined by baseline examination only, and the diagnosis of glaucoma was not definitively confirmed by progressive change over time. Further studies in a larger group of patients with preperimetric glaucoma and studies in a population screening setting are needed.

In conclusion, we have developed a novel method to use OCTA to map and quantify the areas of FPL in glaucoma. The summary parameters, LPA and FPL, provide accurate diagnosis of POAG and have excellent correlation with VF loss both in terms of severity and location. Further studies are needed to evaluate their use in glaucoma screening, staging, predicting progression, and monitoring progression.

References

1. Tham YC, Li X, Wong TY, et al. Global prevalence of glaucoma and projections of glaucoma burden through 2040: a

systematic review and meta-analysis. *Ophthalmology*. 2014;121:2081–2090.
2. Katz J, Quigley HA, Sommer A. Repeatability of the Glaucoma Hemifield Test in automated perimetry. *Invest Ophthalmol Vis Sci*. 1995;36:1658–1664.
3. Lee AC, Sample PA, Blumenthal EZ, et al. Infrequent confirmation of visual field progression. *Ophthalmology*. 2002;109:1059–1065.
4. Leite MT, Zangwill LM, Weinreb RN, et al. Effect of disease severity on the performance of Cirrus spectral-domain OCT for glaucoma diagnosis. *Invest Ophthalmol Vis Sci*. 2010;51:4104–4109.
5. Loewen NA, Zhang X, Tan O, et al. Combining measurements from three anatomical areas for glaucoma diagnosis using Fourier-domain optical coherence tomography. *Br J Ophthalmol*. 2015;99:1224–1229.
6. Tan O, Chopra V, Lu AT, et al. Detection of macular ganglion cell loss in glaucoma by Fourier-domain optical coherence tomography. *Ophthalmology*. 2009;116:2305–2314.e1-2.
7. Lu AT, Wang M, Varma R, et al. Combining nerve fiber layer parameters to optimize glaucoma diagnosis with optical coherence tomography. *Ophthalmology*. 2008;115:1352–1357, 7.e1-2.
8. Medeiros FA, Zangwill LM, Bowd C, et al. Evaluation of retinal nerve fiber layer, optic nerve head, and macular thickness measurements for glaucoma detection using optical coherence tomography. *Am J Ophthalmol*. 2005;139:44–55.
9. Zhang X, Dastiridou A, Francis BA, et al. Comparison of glaucoma progression detection by optical coherence tomography and visual field. *Am J Ophthalmol*. 2017;184:63–74.
10. Kansal V, Armstrong JJ, Pintwala R, Hutnik C. Optical coherence tomography for glaucoma diagnosis: an evidence based meta-analysis. *PLoS One*. 2018;13:e0190621.
11. Wang DL, Raza AS, de Moraes CG, et al. Central glaucomatous damage of the macula can be overlooked by conventional OCT retinal nerve fiber layer thickness analyses. *Transl Vis Sci Technol*. 2015;4:4.
12. Banegas SA, Anton A, Morilla A, et al. Evaluation of the retinal nerve fiber layer thickness, the mean deviation, and the visual field index in progressive glaucoma. *J Glaucoma*. 2016;25:e229–e235.
13. Bowd C, Zangwill LM, Weinreb RN, et al. Estimating optical coherence tomography structural measurement floors to improve detection of progression in advanced glaucoma. *Am J Ophthalmol*. 2017;175:37–44.
14. Mwanza JC, Kim HY, Budenz DL, et al. Residual and dynamic range of retinal nerve fiber layer thickness in glaucoma: comparison of three OCT platforms. *Invest Ophthalmol Vis Sci*. 2015;56:6344–6351.
15. Mwanza JC, Budenz DL, Warren JL, et al. Retinal nerve fibre layer thickness floor and corresponding functional loss in glaucoma. *Br J Ophthalmol*. 2015;99:732–737.
16. Alnawaiseh M, Lahme L, Muller V, et al. Correlation of flow density, as measured using optical coherence tomography angiography, with structural and functional parameters in glaucoma patients. *Graefes Arch Clin Exp Ophthalmol*. 2018;256:589–597.
17. Jia Y, Wei E, Wang X, et al. Optical coherence tomography angiography of optic disc perfusion in glaucoma. *Ophthalmology*. 2014;121:1322–1332.
18. Liu L, Jia Y, Takusagawa HL, et al. Optical coherence tomography angiography of the peripapillary retina in glaucoma. *JAMA Ophthalmol*. 2015;133:1045–1052.
19. Chen CL, Bojikian KD, Wen JC, et al. Peripapillary retinal nerve fiber layer vascular microcirculation in eyes with glaucoma and single-hemifield visual field loss. *JAMA Ophthalmol*. 2017;135:461–468.
20. Yarmohammadi A, Zangwill LM, Manalastas PIC, et al. Peripapillary and macular vessel density in patients with primary open-angle glaucoma and unilateral visual field loss. *Ophthalmology*. 2018;125:578–587.
21. Liu L, Edmunds B, Takusagawa H, et al. Projection-resolved optical coherence tomography angiography of the peripapillary retina in glaucoma. *Am J Ophthalmol*. 2019;207:99–109.
22. Penteado RC, Zangwill LM, Daga FB, et al. Optical coherence tomography angiography macular vascular density measurements and the central 10-2 visual field in glaucoma. *J Glaucoma*. 2018;27:481–489.
23. Takusagawa HL, Liu L, Ma KN, et al. Projection-resolved optical coherence tomography angiography of macular retinal circulation in glaucoma. *Ophthalmology*. 2017;124:1589–1599.
24. Mammo Z, Heisler M, Balaratnasingam C, et al. Quantitative optical coherence tomography angiography of radial peripapillary capillaries in glaucoma, glaucoma suspect, and normal eyes. *Am J Ophthalmol*. 2016;170:41–49.
25. Yarmohammadi A, Zangwill LM, Diniz-Filho A, et al. Optical coherence tomography angiography vessel density in healthy, glaucoma suspect, and glaucoma eyes. *Invest Ophthalmol Vis Sci*. 2016;57:OCT451-459.
26. Yarmohammadi A, Zangwill LM, Diniz-Filho A, et al. Relationship between optical coherence tomography angiography vessel density and severity of visual field loss in glaucoma. *Ophthalmology*. 2016;123:2498–2508.
27. Asrani S, Edghill B, Gupta Y, Meerhoff G. Optical coherence tomography errors in glaucoma. *J Glaucoma*. 2010;19:237–242.
28. Ray R, Stinnett SS, Jaffe GJ. Evaluation of image artifact produced by optical coherence tomography of retinal pathology. *Am J Ophthalmol*. 2005;139:18–29.
29. Hoh ST, Lim MC, Seah SK, et al. Peripapillary retinal nerve fiber layer thickness variations with myopia. *Ophthalmology*. 2006;113:773–777.
30. Zhang X, Parrish 2nd RK, Greenfield DS, et al. Predictive factors for the rate of visual field progression in the Advanced Imaging for Glaucoma Study. *Am J Ophthalmol*. 2019;202:62–71.
31. Zhang X, Dastiridou A, Francis BA, et al. Baseline Fourier-domain optical coherence tomography structural risk factors for visual field progression in the advanced imaging for glaucoma study. *Am J Ophthalmol*. 2016;172:94–103.
32. Jia Y, Tan O, Tokayer J, et al. Split-spectrum amplitude-decorrelation angiography with optical coherence tomography. *Opt Express*. 2012;20:4710–4725.
33. Kraus MF, Potsaid B, Mayer MA, et al. Motion correction in optical coherence tomography volumes on a per A-scan basis using orthogonal scan patterns. *Biomed Opt Express*. 2012;3:1182–1199.
34. Camino A, Zhang M, Gao SS, et al. Evaluation of artifact reduction in optical coherence tomography angiography with real-time tracking and motion correction technology. *Biomed Opt Express*. 2016;7:3905–3915.
35. Zhang M, Wang J, Pechauer AD, et al. Advanced image processing for optical coherence tomographic angiography of macular diseases. *Biomed Opt Express*. 2015;6:4661–4675.
36. Gao SS, Jia Y, Liu L, et al. Compensation for reflectance variation in vessel density quantification by optical coherence tomography angiography. *Invest Ophthalmol Vis Sci*. 2016;57:4485–4492.

37. Zhou X-H, McClish DK, Obuchowski NA. *Statistical Methods in Diagnostic Medicine*. Vol. 569. Hoboken, NJ: John Wiley & Sons; 2009.
38. Hodapp E, Parrish RK, Anderson DR. *Clinical Decisions in Glaucoma*. St Louis: Mosby; 1993:52–61.
39. Rao HL, Pradhan ZS, Weinreb RN, et al. Regional comparisons of optical coherence tomography angiography vessel density in primary open-angle glaucoma. *Am J Ophthalmol*. 2016;171:75–83.
40. Allegrini D, Montesano G, Fogagnolo P, et al. The volume of peripapillary vessels within the retinal nerve fibre layer: an optical coherence tomography angiography study of normal subjects. *Br J Ophthalmol*. 2018;102:611–621.
41. Le PV, Tan O, Chopra V, et al. Regional correlation among ganglion cell complex, nerve fiber layer, and visual field loss in glaucoma. *Invest Ophthalmol Vis Sci*. 2013;54:4287–4295.
42. Garway-Heath DF, Poinoosawmy D, Fitzke FW, Hitchings RA. Mapping the visual field to the optic disc in normal tension glaucoma eyes. *Ophthalmology*. 2000;107:1809–1815.
43. Scripsema NK, Garcia PM, Bavier RD, et al. Optical coherence tomography angiography analysis of perfused peripapillary capillaries in primary open-angle glaucoma and normal-tension glaucoma. *Invest Ophthalmol Vis Sci*. 2016;57. OCT611-620.
44. Richter GM, Sylvester B, Chu Z, et al. Peripapillary microvasculature in the retinal nerve fiber layer in glaucoma by optical coherence tomography angiography: focal structural and functional correlations and diagnostic performance. *Clin Ophthalmol*. 2018;12:2285–2296.
45. Yarmohammadi A, Zangwill LM, Diniz-Filho A, et al. Peripapillary and macular vessel density in patients with glaucoma and single-hemifield visual field defect. *Ophthalmology*. 2017;124:709–719.
46. Zhang X, Loewen N, Tan O, et al. Predicting development of glaucomatous visual field conversion using baseline Fourier-domain optical coherence tomography. *Am J Ophthalmol*. 2016;163:29–37.

Footnotes and Financial Disclosures

Originally received: June 20, 2019.
Final revision: October 24, 2019.
Accepted: October 30, 2019.
Available online: November 8, 2019. Manuscript no. 2019-1339.

Casey Eye Institute and Department of Ophthalmology, Oregon Health and Science University, Portland, Oregon.

*Both authors A.C. and L.L. are co-first authors and contributed equally to this study.

Financial Disclosure(s):
The author(s) have made the following disclosure(s): Oregon Health & Science University, Y.J., and D.H. have financial interest in Optovue, Inc., a company that may have a commercial interest in the results of this research and technology. These potential conflicts of interest have been reviewed and are managed by Oregon Health & Science University. The other authors do not report any potential financial conflicts of interest.

Supported by National Institutes of Health Grants R01 EY023285, P30 EY010572, and R01 EY010145, and unrestricted departmental funding from Research to Prevent Blindness (New York, NY). The sponsor or funding organization had no role in the design or conduct of this research.

HUMAN SUBJECTS: Human subjects were included in this study. The human ethics committees at the Oregon Health & Science University approved the study. All research adhered to the tenets of the Declaration of Helsinki. All participants provided informed consent.

No animal subjects were used in this study.

Author Contributions:

Conception and design: Chen, Liu, Edmunds, Lombardi, Davis, Morrison, Jia, Huang

Data collection: Chen, Liu, Edmunds, Lombardi, Davis, Morrison, Jia, Huang

Analysis and interpretation: Chen, Liu, Wang, Zang, Edmunds, Lombardi, Davis, Morrison, Huang

Obtained funding: Jia, Huang

Overall responsibility: Chen, Liu, Wang, Zang, Jia, Huang

Abbreviations and Acronyms:
CD = capillary density; **D** = diopters; **dB** = decibels; **FPL** = focal perfusion loss; **LPA** = low perfusion area; **MD** = mean deviation; **NFL** = nerve fiber layer; **NFLP** = nerve fiber layer plexus; **OCTA** = OCT angiography; **ONH** = optic nerve head; **POAG** = primary open-angle glaucoma; **VF** = visual field.

Correspondence:
David Huang, MD, PhD, Casey Eye Institute, Oregon Health & Science University, 3375 S.W. Terwilliger Blvd., Portland, OR 97239-4197. E-mail: davidhuang@alum.mit.edu.